Changes in orographic precipitation patterns caused by a shift from snow to rain

Tamlin M. Pavelsky,[1] Stefan Sobolowski,[2] Sarah B. Kapnick,[3,4] and Jason B. Barnes[1]

Received 14 June 2012; revised 7 August 2012; accepted 8 August 2012; published 25 September 2012.

[1] Climate warming will likely cause a shift from snow to rain in midlatitude mountains. Because rain falls faster than snow, it is not advected as far by prevailing winds before reaching the ground. A shift in precipitation phase thus may alter precipitation patterns. Using the Weather Research and Forecasting (WRF) regional climate model at 27-9-3 km resolutions over the California Sierra Nevada, we conducted an idealized experiment consisting of a present climate control run and two additional simulations in which (a) fall speed for snow is similar to rain and (b) all precipitation is constrained to fall as liquid. Rather than simulating future climates directly, these perturbation experiments allow us to test the potential impacts of changing precipitation phase in isolation from other factors such as variable large-scale atmospheric circulation. Relative to the control, both perturbations result in a rain shadow deepened by ∼30–60%, with increased focusing of precipitation on the western Sierra Nevada slopes best resolved at ≤9 km resolutions. Our results suggest that altered precipitation phase associated with climate change will likely affect spatial distributions of water resources, floods, and landslides in the Sierra Nevada and similar midlatitude mountain ranges. **Citation:** Pavelsky, T. M., S. Sobolowski, S. B. Kapnick, and J. B. Barnes (2012), Changes in orographic precipitation patterns caused by a shift from snow to rain, *Geophys. Res. Lett.*, *39*, L18706, doi:10.1029/2012GL052741.

1. Introduction

[2] Precipitation in mountains is a critical component of global freshwater resources. Many regions, including the western United States, are particularly dependent on mountain precipitation because high-elevation snowpacks provide a natural reservoir that stores water during the winter and later releases it via spring snowmelt [*Barnett et al.*, 2005]. Among the regions most dependent on mountain snowpack is California, where snowfall in the Sierra Nevada provides the majority of water to agricultural areas in the San Joaquin Valley and large portions of the water necessary to support the metropolitan areas of San Francisco and Los Angeles [*Villaraigosa*, 2008; *Wang et al.*, 2011]. Over the last few decades, many studies have highlighted the vulnerability of this natural reservoir to future climate change [*Barnett et al.*, 2008; *Cayan et al.*, 2008; *Hayhoe et al.*, 2004; *Kapnick and Hall*, 2012; *Lettenmaier and Gan*, 1990]. More precipitation will fall as rain instead of snow as temperatures warm, and snowmelt will occur earlier in the year. Already, earlier snowpack melt in the Sierra Nevada consistent with anthropogenic forcing has been observed [*Hidalgo et al.*, 2009; *Kapnick and Hall*, 2010]. In the Sierra Nevada, snow is advected deep into the mountain range by the prevailing westerlies before reaching the land surface. However, rain falls at approximately an order of magnitude higher velocity than snow [*Ferrier*, 1994; *Thompson et al.*, 2008]. In theory, a shift from snow to rain should reduce this advection length scale and thus alter the spatial patterns of montane precipitation. This concept has been tested using simplified atmospheric models on geologic time scales, and results suggest that such a shift can have major impacts on mountain range morphology [*Anders et al.*, 2008]. Spatial patterns of precipitation consistent with this mechanism have been observed in future climate simulations of central Colorado [*Rasmussen et al.*, 2011], but the potential impact of changing precipitation phase, in isolation from other climate influences (e.g., altered large-scale atmospheric dynamics [*Gao et al.*, 2012]), remains untested.

[3] Although consensus exists that anthropogenic climate change will lead to a major shift in snowmelt timing in the Sierra Nevada, previous global climate model (GCM) studies of changes in total precipitation, which often involve using statistical or dynamical downscaling to enhance model resolution, do not observe a consistent signal [*Barnett et al.*, 2008; *Cayan et al.*, 2008; *Maurer*, 2007]. In part, this uncertainty is likely due to fundamental deficiencies in accurately simulating precipitation patterns and trends in global and regional climate models [*Benestad et al.*, 2012; *Stephens et al.*, 2010]. To address this uncertainty, pioneering approaches are modifying present-day observations as model boundary conditions to examine the potential impacts of warming on precipitation [*Rasmussen et al.*, 2011]. Another more direct approach is to explore the effects of specific physical changes on regional precipitation patterns: we (a) downscale reanalysis data using a regional climate model, (b) validate the simulated precipitation against observations, and (c) rerun the model with perturbed model physics consistent with expected changes to future climate conditions.

2. Methods

[4] We performed three regional modeling experiments using the Weather Research and Forecasting (WRF) model

[1]Department of Geological Sciences, University of North Carolina at Chapel Hill, Chapel Hill, North Carolina, USA.
[2]Uni Bjerknes Centre for Climate Research, Bergen, Norway.
[3]Atmospheric and Oceanic Sciences Program, Princeton University, Princeton, New Jersey, USA.
[4]NOAA Geophysical Fluid Dynamics Laboratory, Princeton, New Jersey, USA.

Corresponding author: T. M. Pavelsky, Department of Geological Sciences, University of North Carolina at Chapel Hill, Chapel Hill, NC 27599, USA. (pavelsky@unc.edu)

0094-8276/12/2012GL052741

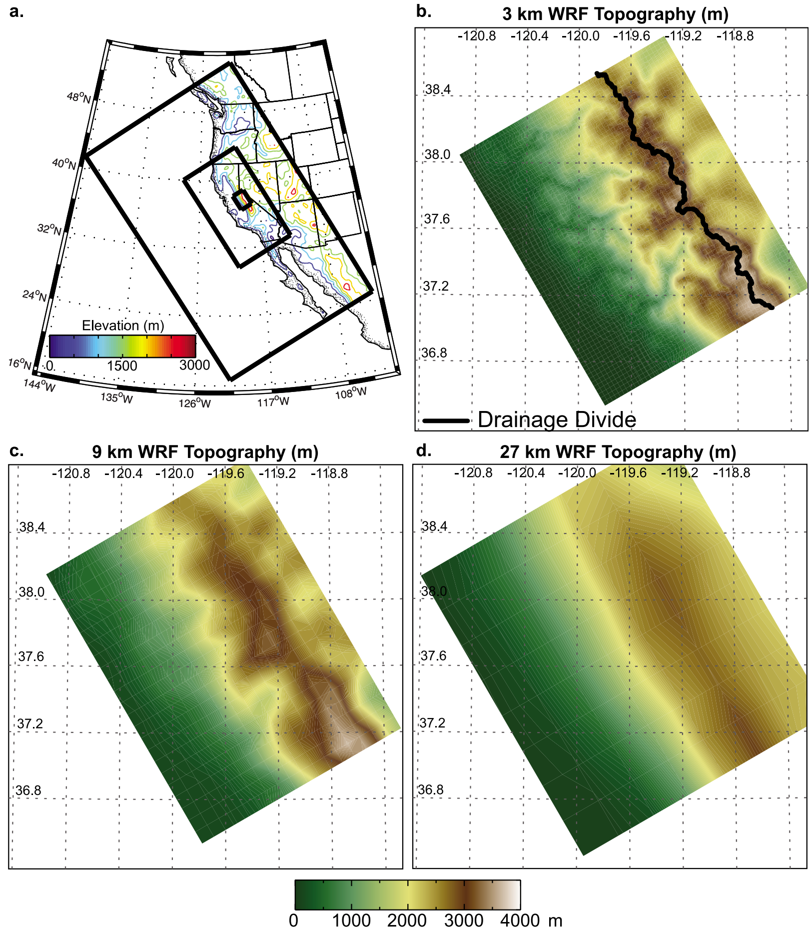

Figure 1. Sierra Nevada model topography. (a) Areas covered by the 3, 9, and 27 km WRF domains, and (b–d) the 3-km domain area topography at decreasing spatial resolution. Black line in b is the drainage divide.

v. 3.1.1 [*Skamarock et al.*, 2008] for water year 2002 (October 2001–September 2002). Each experiment was run using three nested domains at increasingly finer spatial resolutions (27, 9, and 3 km) to assess how differences in the representation of orography and other spatially dependent processes affect changes in precipitation patterns (Figure 1). These domains are referred to as D27, D9, and D3, respectively. The first run is a control experiment designed to represent present day conditions over the Sierra Nevada, while the second and third are perturbation experiments. Spatial patterns of precipitation in the control run have been validated against *in situ* observations in a previous study, in which the full model setup is described in detail [*Pavelsky et al.*, 2011]. The experiments employ identical model specifications and boundary conditions from the North American Regional Reanalysis [*Mesinger et al.*, 2006]; the only differences between the three are alterations made to the microphysics scheme under the perturbation scenarios.

[5] The first perturbation experiment (‘high fall speed’, FS) is defined by an alteration to the cloud microphysics scheme that approximates the effect of a change in hydrometeor phase to all rain by modifying the fall speeds of snow and graupel. The Thompson cloud microphysics scheme [*Thompson et al.*, 2008] chosen for these experiments calculates terminal fall speed as a function of hydrometeor diameter. We change the coefficients in the fall speed equations for graupel and snow to match those of rain, with maximum fall speed capped at 7.3 m/s [*Ferrier*, 1994]. The FS experiment was also run for several months with a maximum fall speed of 4.5 m/s, with only minor differences in precipitation patterns compared to the experiment included here. While this is an idealized perturbation, it effectively sets an upper boundary on the potential effects of a phase transition from predominantly frozen to predominantly liquid precipitation. Moreover, it isolates the potential effect of this change from other influences of changing climate such as seasonal changes in precipitation and land surface changes. The second perturbation experiment (‘rain only’, RO) also aims to simulate a change in hydrometeor phase to all rain. In this instance the moisture phase conversion from liquid to solid phase are switched off in the microphysics scheme so that all precipitation falls as rain. The RO experiment provides a useful comparison to the more extreme FS case by removing the potentially spurious influence of fast-falling frozen species. These experiments combine to isolate the potential effect of precipitation phase from other influences of changing climate such as seasonal changes, land surface changes and radiatively-induced constraints on precipitation [*Stephens and Ellis*, 2008].

[6] The analytical approach is straightforward and involves direct comparison of the perturbed simulations to the control experiment. We also examine average cross

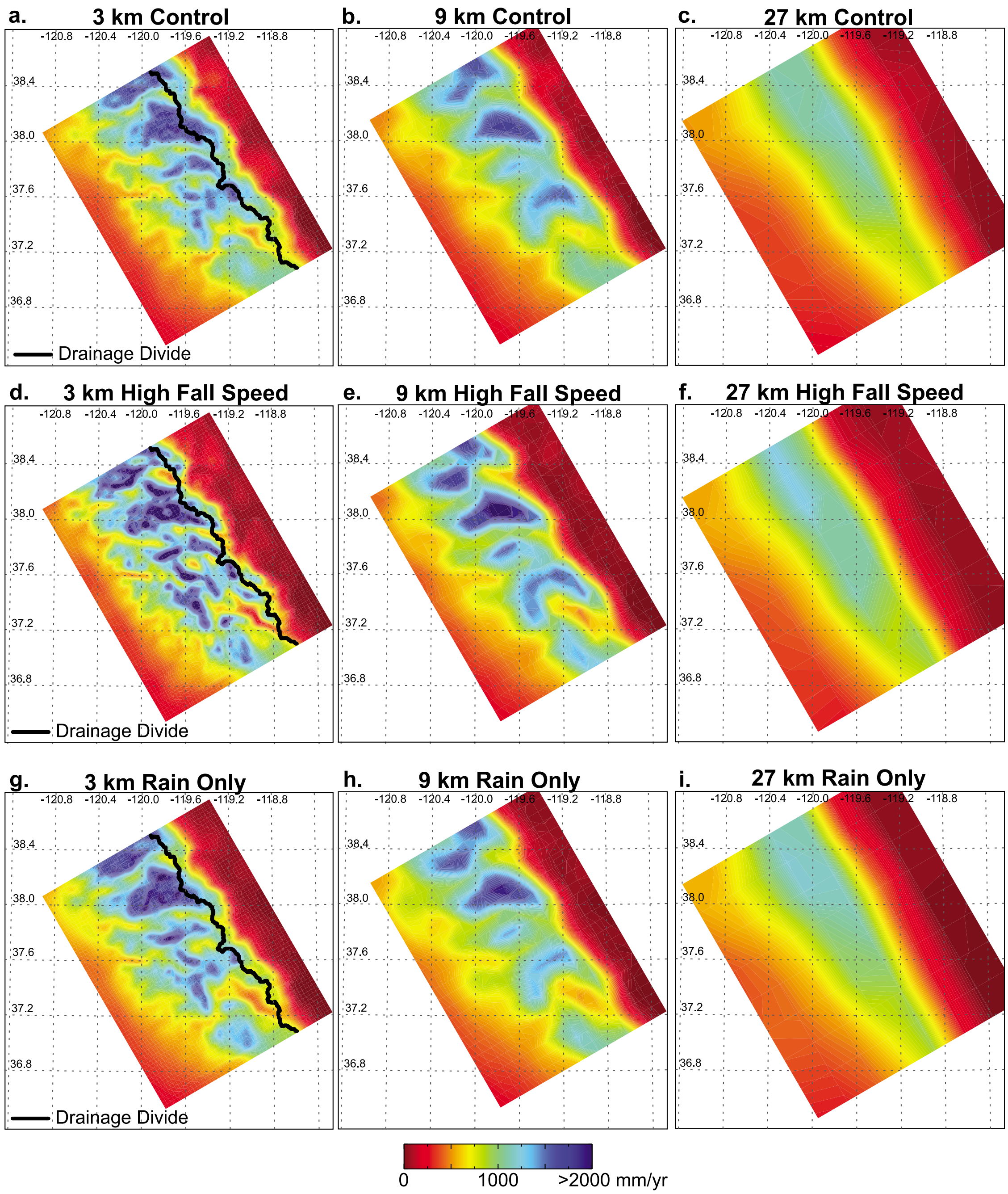

Figure 2. Simulated annual precipitation (mm/yr) for the 3-km domain area at 3, 9, and 27 km spatial resolutions (Figure 1). (a–c) Mean water year 2002 total annual precipitation from the control experiment at 3, 9, and 27 km. (d–f) Precipitation from the high fall speed experiment (FS), and (g–i) precipitation for the rain-only experiment (RO). Precipitation values in Figures 2d–2i are calibrated so that mean precipitation matches the control experiment for the equivalent resolution.

sections of precipitation change across the Sierra Nevada. Because the model grid orientation is designed to parallel the across-strike direction of the Sierra Nevada, we simply calculate average precipitation change for every column of grid cells in each domain. Total precipitation change on either side of the principal drainage divide in the Sierra Nevada (black line, Figures 1b, 2, and 3) is also calculated. In order to ensure hydrologic fidelity, the drainage boundary was calculated from the Hydrosheds dataset [*Lehner et al.*, 2008]. This boundary was intersected with the D3 grid using ArcGIS to divide the grid cells into those draining east and draining west.

3. Results

[7] Results for spatial patterns of precipitation under present-day conditions show the importance of model resolution, and thus orographic variability, in simulating both total precipitation and its spatial patterns (Figures 2a–2c). In all domains, precipitation is correlated with elevation but

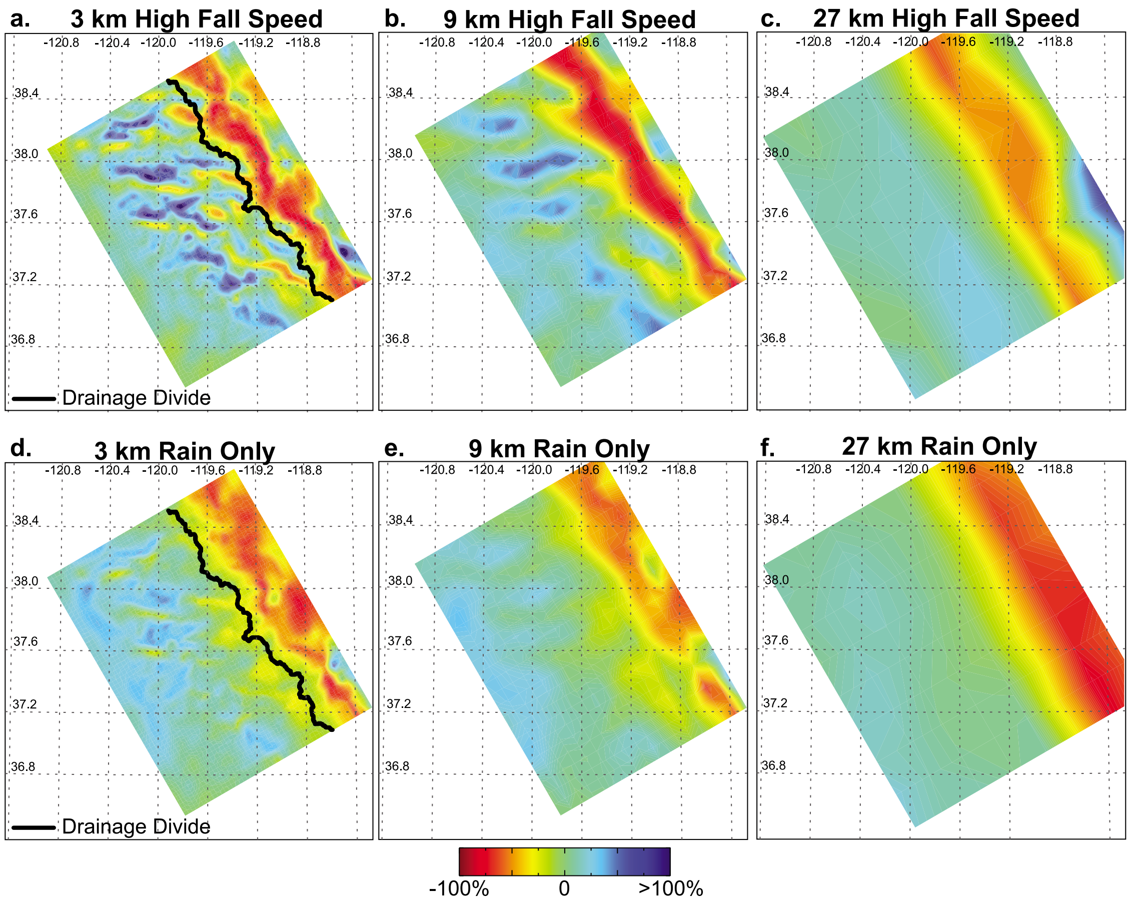

Figure 3. Changes in precipitation patterns in % relative to the control run. (a–c) Difference between total annual precipitation from the control experiment and the high fall speed experiment, expressed as a percent of the control experiment at 3, 9, and 27 km resolutions. (d–f) The same for the rain-only experiment. Precipitation values are calibrated so that mean precipitation matches the control experiment for the equivalent resolution.

also exhibits a north-south gradient, with the higher precipitation in the north associated with large-scale patterns of atmospheric circulation. The western (windward) flank of the range receives substantially more precipitation than the eastern (leeward) flank. Mean 2001–2002 total precipitation values (Table 1) show higher precipitation at higher spatial resolution. Previous work indicates that D3 precipitation exhibits the smallest mean bias relative to *in situ* measurements [*Pavelsky et al.*, 2011].

[8] Broad-scale precipitation patterns are similar in the FS experiment and the control run, but there are key differences (Figures 2d–2f). Because our main focus is on variations in spatial patterns of precipitation rather than absolute values, we calibrate the FS and RO precipitation grids such that the mean precipitation value is identical to the control run for the corresponding model domain in the D3 region. Precipitation becomes more focused in the FS experiment, with expanded areas of very high precipitation (>2000 mm/yr) on the western range flank and a drier rain shadow on the eastern flank (Figure 2). Mean domain-averaged precipitation in all domains is similar to the control run (Table 1). However, precipitation is ~10% greater in the FS experiment in D3, while precipitation declines by ~10% in D27. We hypothesize that the increase in precipitation at high resolutions and decreased precipitation at low resolutions are associated with the resolution dependence of precipitation advection with respect to orographic height, but the precise mechanism merits further investigation.

[9] The large-scale spatial patterns of precipitation in the RO experiment also show increased precipitation focused

Table 1. Mean Precipitation Values (mm/yr) for the Three Experiments[a]

	Control				High Fall Speed (FS)				Rain Only (RO)			
	Mean	West	East	E/W	Mean	West	East	E/W	Mean	West	East	E/W
D3	986	1191	438	0.37	1034	1347(1284)	198(188)	0.15	668	846(1249)	193(284)	0.23
D9	894	1102	338	0.31	880	1150(1168)	157(159)	0.14	577	733(1136)	160(248)	0.22
D27	723	895	265	0.3	632	820(938)	130(148)	0.16	471	604(927)	115(177)	0.19

[a]For each experiment, precipitation values are provided for the entire D3 area (Figure 1) and separately for the regions west and east of the drainage divide, along with the ratio between the two (E/W). Values in parentheses are calibrated so that mean precipitation matches the control experiment.

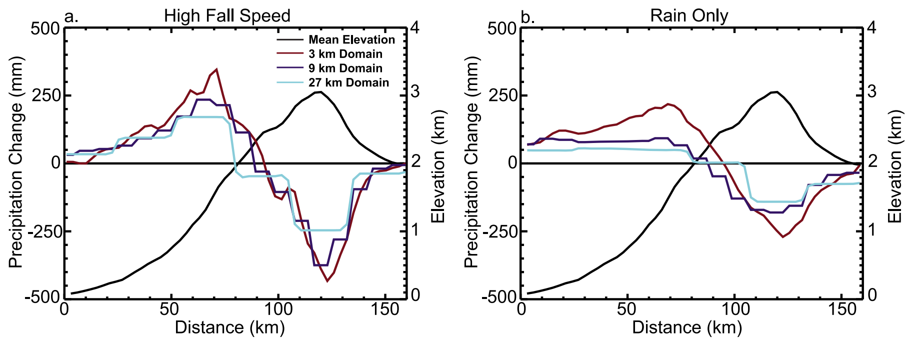

Figure 4. Orographic precipitation change relative to mean topography across the central Sierra Nevada (3-km model domain in Figure 1). (a) Difference in mean water year 2002 precipitation between the high fall speed experiment and the control experiment. (b) Same for the rain-only experiment. Precipitation values are calibrated so that mean precipitation matches the control experiment at the equivalent resolution.

on the western flank relative to the eastern flank (Figure 3). The key difference is that annual precipitation is, on average, ~30% lower than in the control run (Table 1). This difference is likely related to simulation of hydrometeor formation mechanisms in the microphysics parameterization [*Thompson et al.*, 2008]. By excluding the conversion between liquid and solid species in forcing all precipitation to fall as rain, we have eliminated a key mechanism for hydrometeor development, the growth of cloud ice and water droplets through riming and collision. Vertical profiles of water vapor (see auxiliary material, Figure S1)[1] are very similar in the control and RO runs, while cloud water content is substantially higher in the RO run. This suggests that condensation processes do not change substantially but that precipitation becomes much less efficient in the RO run. This effect may be either a byproduct of the model parameterization or a possible impact of future warming-induced precipitation phase change. There is some indication that precipitation efficiency decreases during large atmospheric river events in California at temperatures higher than 0°C [*Guan et al.*, 2010]. If the atmospheric arm of the hydrological cycle slows down [*Held and Soden*, 2006] and precipitation efficiency decreases [*Stephens and Ellis*, 2008], then the potential effects due to phase change shown here may also be exacerbated. Regardless of whether the reduction in precipitation is a real effect, the RO experiment allows us to isolate and verify the changes in spatial distribution of precipitation found in the FS experiment. Both experiments yield similar results when normalized by the control run (Table 1 and Figure 4).

[10] A large reduction in precipitation east of the drainage divide is evident at all model resolutions in both perturbation experiments (Figures 3 and 4). In the control run, the ratio of precipitation on the east and west sides of the drainage divide is 0.30–0.37, decreasing to 0.14–0.23 in the perturbation experiments depending on model resolution and perturbation type (Table 1). This corresponds to a deepening of the rain shadow by ~30–60%. Compared to the RO experiment, the FS experiment results in slightly stronger deepening of the rain shadow (Figure 4). West of the divide, both experiments show higher precipitation along ridges than in valleys at high spatial resolutions (Figures 3a and 3d). In particular, the FS experiment suggests that a shift from snow to rain would likely increase the focusing of precipitation on favorably oriented hillslopes, with a maximum increase in precipitation of ~120% in D3. The RO experiment shows similar but more muted results when the influence of the overall precipitation decrease is removed (Figure 4). Elevated precipitation on the western flank decreases with coarsening model resolution (e.g., D27), suggesting that it is a function of more detailed orographic forcing at higher resolutions.

4. Discussion and Conclusions

[11] The fact that both perturbation experiments produce similar results despite representing very different changes to model physics suggests that the response of spatial precipitation patterns to changing fall speed associated with a shift from frozen to liquid precipitation is not an artifact of a particular model parameterization. Strengthening of the rain shadow is therefore likely a fundamental response to changing precipitation phase. Our results suggest that altered precipitation patterns cannot be fully captured at resolutions greater than ~27 km, where mountain precipitation is substantially underestimated [*Pavelsky et al.*, 2011] and detailed patterns of orography cannot be resolved (Figure 3). Instead, the impacts of changing precipitation phase in mountain regions can be better achieved at resolutions of ~9 or, preferably, ~3 km. While regional climate model studies have been conducted with resolutions near 3 km [*Pavelsky et al.*, 2011; *Rasmussen et al.*, 2011], climate studies using GCMs and RCMs have generally used coarser resolutions (often ≥50 km) or statistical downscaling methods, which would be unlikely to capture all observed changes in spatial precipitation patterns due to the smoothing of orography at lower resolutions (Figure 1).

[12] In warming climates, a change in precipitation phase and fall speed is likely to vary depending on altitude, topography, atmospheric circulation, and time of year, and our results do not capture this variability. Full conversion from snow to rain, as simulated here, is unlikely to occur in the foreseeable future. However, as temperatures increase through the 21st century and beyond, a major shift from snowfall to rainfall in the Western U.S. is anticipated [*Rasmussen et al.*, 2011; *Wi et al.*, 2012]. The greatest shifts in the next century are likely to occur below 3000 m, where

[1]Auxiliary materials are available in the HTML. doi:10.1029/2012GL052741.

>80% of snowpack storage currently occurs in the Sierra Nevada (e.g., Figure 4) [*Cayan et al.*, 2008; *Hayhoe et al.*, 2004]. An increase in western Sierra Nevada liquid precipitation may offer a modest increase in water resources to the Central Valley of California, though positive impacts would be complicated by a predicted change in seasonality of streamflow from snowmelt-driven summertime flow to wintertime stormflow [*Wang et al.*, 2011]. Conversely, a decrease in precipitation in the eastern Sierra Nevada could dramatically affect water resource availability for Los Angeles, which receives ~35% of its water supply from the Owens Valley via the Los Angeles Aqueduct [*Villaraigosa*, 2008].

[13] An increasing focus of rain on windward hillslopes could exacerbate flash flood risk and influence the timing and prevalence of landslides, which are often triggered by focused precipitation [*Crozier*, 2010]. These changes could have a substantial impact on human infrastructure in the Sierra Nevada, including roads. Increased risk would occur with a shift from snow to rain even if precipitation patterns stayed identical to today, but the changing spatial patterns indicated here would exacerbate the problem (e.g., Figure 3). These changes could also have a large impact on Sierra Nevada ecosystems, which are closely tied to the form and quantity of precipitation [*Lloyd and Graumlich*, 1997]. As precipitation phase shifts, spatial patterns of plant and animal habitat may be disrupted to a greater extent than would be predicted from an increase in temperature alone.

[14] Because precipitation phase is so closely tied to temperature, altered precipitation patterns due to a change from snow to rain are also likely to occur in other midlatitude mountain ranges under climate change scenarios. Mountain ranges most likely to be affected are those with wintertime temperatures close to 0°C and a dominant prevailing wind direction [*Anders et al.*, 2008]. Other regions where a precipitation phase change could cause similar shifts in spatial precipitation patterns include the U.S. Cascades, the Patagonian Andes, Scandinavia, and the European Alps.

[15] **Acknowledgments.** We thank the Renaissance Computing Institute (RENCI) in Chapel Hill, NC for providing access to high-performance computing resources. We also thank three anonymous reviewers for their useful comments.

[16] The Editor thanks the anonymous reviewers for their assistance in evaluating this paper.

References

Anders, A. M., G. H. Roe, D. R. Montgomery, and B. Hallet (2008), Influence of precipitation phase on the form of mountain ranges, *Geology*, *36*(6), 479–482, doi:10.1130/G24821A.1.

Barnett, T. P., J. C. Adam, and D. P. Lettenmaier (2005), Potential impacts of a warming climate on water availability in snow-dominated regions, *Nature*, *438*(7066), 303–309, doi:10.1038/nature04141.

Barnett, T. P., et al. (2008), Human-induced changes in the hydrology of the western United States, *Science*, *319*(5866), 1080–1083, doi:10.1126/science.1152538.

Benestad, R. E., D. Nychka, and L. O. Mearns (2012), Spatial and temporally consistent prediction of heavy precipitation from mean values, *Nat. Clim. Change*, *2*(7), 544–547.

Cayan, D. R., E. P. Maurer, M. D. Dettinger, M. Tyree, and K. Hayhoe (2008), Climate change scenarios for the California region, *Clim. Change*, *87*(S1), 21–42, doi:10.1007/s10584-007-9377-6.

Crozier, M. J. (2010), Deciphering the effect of climate change on landslide activity: A review, *Geomorphology*, *124*(3–4), 260–267, doi:10.1016/j.geomorph.2010.04.009.

Ferrier, B. S. (1994), A double-moment multiple-phase 4-class bulk ice scheme: 1. Description, *J. Atmos. Sci.*, *51*(2), 249–280, doi:10.1175/1520-0469(1994)051<0249:ADMMPF>2.0.CO;2.

Guan, B., N. P. Molotch, D. E. Waliser, E. J. Fetzer, and P. J. Neiman (2010), Extreme snowfall events linked to atmospheric rivers and surface air temperature via satellite measurements, *Geophys. Res. Lett.*, *37*, L20401, doi:10.1029/2010GL044696.

Gao, Y., L. R. Leung, E. P. Salathé, F. Dominguez, B. Nijssen, and D. P. Lettenmaier (2012), Moisture flux convergence in regional and global climate models: Implications for droughts in the southwestern United States under climate change, *Geophys. Res. Lett.*, *39*, L09711, doi:10.1029/2012GL051560.

Hayhoe, K., et al. (2004), Emissions pathways, climate change, and impacts on California, *Proc. Natl. Acad. Sci. U. S. A.*, *101*(34), 12,422–12,427, doi:10.1073/pnas.0404500101.

Held, I. M., and B. J. Soden (2006), Robust responses of the hydrologic cycle to global warming, *J. Clim.*, *19*, 5686–5699, doi:10.1175/JCLI3990.1.

Hidalgo, H. G., et al. (2009), Detection and attribution of streamflow timing changes to climate change in the western United States, *J. Clim.*, *22*(13), 3838–3855, doi:10.1175/2009JCLI2470.1.

Kapnick, S., and A. Hall (2010), Observed climate-snowpack relationships in California and their implications for the future, *J. Clim.*, *23*(13), 3446–3456, doi:10.1175/2010JCLI2903.1.

Kapnick, S., and A. Hall (2012), Causes of recent changes in western North American snowpack, *Clim. Dyn.*, *38*(9–10), 1885–1899, doi:10.1007/s00382-011-1089-y.

Lehner, B. L., K. Verdin, and A. Jarvis (2008), New global hydrography derived from spaceborne elevation data, *Eos Trans. AGU*, *89*(10), 93, doi:10.1029/2008EO100001.

Lettenmaier, D. P., and T. Y. Gan (1990), Hydrologic sensitivities of the Sacramento–San Joaquin River Basin, California, to global warming, *Water Resour. Res.*, *26*(1), 69–86, doi:10.1029/WR026i001p00069.

Lloyd, A. H., and L. J. Graumlich (1997), Holocene dynamics of treeline forests in the Sierra Nevada, *Ecology*, *78*(4), 1199–1210, doi:10.1890/0012-9658(1997)078[1199:HDOTFI]2.0.CO;2.

Maurer, E. P. (2007), Uncertainty in hydrologic impacts of climate change in the Sierra Nevada, California, under two emissions scenarios, *Clim. Change*, *82*(3–4), 309–325, doi:10.1007/s10584-006-9180-9.

Mesinger, F., et al. (2006), North American regional reanalysis, *Bull. Am. Meteorol. Soc.*, *87*(3), 343–360, doi:10.1175/BAMS-87-3-343.

Pavelsky, T. M., S. Kapnick, and A. Hall (2011), Accumulation and melt dynamics of snowpack from a multiresolution regional climate model in the central Sierra Nevada, California, *J. Geophys. Res.*, *116*, D16115, doi:10.1029/2010JD015479.

Rasmussen, R., et al. (2011), High-resolution coupled climate runoff simulations of seasonal snowfall over Colorado: A process study of current and warmer climate, *J. Clim.*, *24*(12), 3015–3048, doi:10.1175/2010JCLI3985.1.

Skamarock, W. C., J. B. Klemp, J. Dudhia, D. O. Gill, D. M. Barker, M. Duda, X. Huang, W. Wang, and J. G. Powers (2008), A description of the Advanced Research WRF version 3, report, Natl. Cent. for Atmos. Res., Boulder, Colo.

Stephens, G. L., and T. D. Ellis (2008), Controls of global-mean precipitation increases in global warming GCM experiments, *J. Clim.*, *21*, 6141–6155, doi:10.1175/2008JCLI2144.1.

Stephens, G. L., T. L'Ecuyer, R. Forbes, A. Gettlemen, J.-C. Golaz, A. Bodas-Salcedo, K. Suzuki, P. Gabriel, and J. Haynes (2010), Dreary state of precipitation in global models, *J. Geophys. Res.*, *115*, D24211, doi:10.1029/2010JD014532.

Thompson, G., P. R. Field, R. M. Rasmussen, and W. D. Hall (2008), Explicit forecasts of winter precipitation using an improved bulk microphysics scheme. Part II: Implementation of a new snow parameterization, *Mon. Weather Rev.*, *136*(12), 5095–5115, doi:10.1175/2008MWR2387.1.

Villaraigosa, A. R. (2008), Securing L.A.'s water supply, 32 pp., Dep. of Water and Power, Los Angeles, Calif.

Wang, J., H. Yin, and F. Chung (2011), Isolated and integrated effects of sea level rise, seasonal runoff shifts, and annual runoff volume on California's largest water supply, *J. Hydrol.*, *405*(1–2), 83–92, doi:10.1016/j.jhydrol.2011.05.012.

Wi, S., F. Dominguez, M. Durcik, J. Valdes, H. F. Diaz, and C. L. Castro (2012), Climate change projection of snowfall in the Colorado River Basin using dynamical downscaling, *Water Resour. Res.*, *48*, W05504, doi:10.1029/2011WR010674.